Korean J. Chem. Eng., 39(7), 1952-1958 (2022)
DOI: 10.1007/s11814-021-1014-y

pISSN: 0256-1115
eISSN: 1975-7220

Thermal and mechanical properties of poly(latic acid) reinforced with silanized basalt scales

Shan-Shan Yao*, Ming-Zhan Gao*, Zhao-Yang Feng, Fan-Long Jin*,†, and Soo-Jin Park***,†**

*Department of Polymer Materials, Jilin Institute of Chemical Technology, Jilin City 132022, P. R. China
**Jilin Jinshi New Material Technology Co., Ltd., No.67 Jianxin Road, Jilin Economic and Technological Development Zone, Jilin City 132101, P. R. China
***Department of Chemistry, Inha University, Michuhol-gu, Incheon 22212, Korea
(*Received 9 September 2021 • Revised 25 October 2021 • Accepted 11 November 2021*)

Abstract−Biodegradable poly(lactic acid) (PLA)-based composites were prepared using PLA and basalt scale (BS) via a solution-blending method. BS surfaces were treated using a silane coupling agent, and their surface properties were characterized by high-resolution scanning electron microscopy, energy-dispersive X-ray spectrometry, and X-ray photoelectron spectrometry. Moreover, the influence of BS content on the thermal properties, flexural properties, impact strength, and morphology of the PLA/silane-coupling-agent-treated BS (KH-BS) composites was analyzed. The thermal stability of the composites significantly increased due to the addition of KH-BS. Impact strength tests showed that the impact strength of the PLA/KH-BS composite with 4 wt% KH-BS was 3.14 kJ/m^2, which is 51% higher than that of pristine PLA (2.07 kJ/m^2). The analysis of the fracture surfaces of the composites after the impact strength tests revealed a rough morphology with numerous river-like micro-cracks. The study results demonstrate that the addition of KH-BS significantly improves the thermal stability and impact strength of PLA/KH-BS composites.

Keywords: Poly(Lactic Acid), Basalt Scale, Composites, Surface Treatment, Impact Strength

INTRODUCTION

Poly(lactic acid) (PLA), a type of thermoplastic aliphatic polyester, exhibits biodegradability and biocompatibility and is consequently considered as one of the most promising bioexplanatory polymer materials in the medical field. It can be synthesized by the direct condensation of lactic acid or ring-opening polymerization of lactide [13]. Moreover, PLA can be degraded into carbon dioxide and water under natural conditions. Furthermore, the rapid enzymatic hydrolysis of PLA can be induced at low temperatures using current techniques. Therefore, PLA and its products are environmentally friendly. PLA products exhibit a good virtuous cycle in nature, without any environmental damage [4-6].

PLA possesses high strength, high hardness, good ductility, electrical conductivity, thermal conductivity, and excellent degradation. Additionally, it has good gloss and transparency that is equivalent to those of polystyrene film. However, PLA has poor thermal stability, high brittleness, and low impact strength, causing serious limitations in numerous application fields [7-10]. The most common strategy for overcoming these shortcomings is preparing PLA composites. PLA composites in either macro or micro can afford novel properties by using physical or chemical methods to form new materials through various processing. PLA composites exhibit superior properties compared to the pristine materials as they exhibit the properties of the different materials in the composites [11-13].

Basalt scale (BS) was prepared through high-temperature melting, clarification, molding, and screening of natural basalt. It has a transparent or bronze colored lamellar structure and is mainly comprised of silicon dioxide, calcium oxide, and iron oxide. Silicon dioxide is the most prominent component of BS, accounting for 45-60% of the total content. It maintains the bending, tensile, compressive, and impact resistances of BS as well as the chemical stability. BS contains 6-12% calcium oxide, which mainly improves the water corrosion resistance of BS, and BS contains 5-15% iron oxide, which is the reason for its bronze color [14-17].

BS is a compact, acid and alkali resistant, with high chemical stability, and inexpensive inorganic additive. It can be used with inorganic adhesives to produce a heat-resistant, flame-retardant coating that can be used at 700 °C. As a new type of scale-like material, BS is environmentally friendly and inexpensive and is employed as an ecofriendly filler to improve the performance of polymers and the wear resistance of polymer coatings [18,19].

Currently, few reports exist on BS-reinforced PLA composites; they mainly focus on the effects of the basalt powder content and basalt fiber length on the mechanical properties of the PLA/basalt powder and PLA/basalt fiber composites, respectively [16,20]. To improve the interfacial compatibility between the basalt powder/fiber and PLA matrix, the surfaces of the basalt powder/fiber are generally treated using coupling agents, acid-base treatments, plasma treatments, and surface coating modifications [21-23]. Herein, to improve the impact strength of PLA, biodegradable PLA/BS composites were prepared using BS as a reinforcing agent through a solution-blending method. Furthermore, BS surfaces were treated using a silane coupling agent, and the surface properties of BS were charac-

†To whom correspondence should be addressed.
E-mail: jinfanlong@163.com, sjpark@inha.ac.kr

terized via high-resolution scanning electron microscopy (HR-SEM), energy-dispersive X-ray spectrometry (EDX), and X-ray photoelectron spectrometry (XPS). The effects of BS content on the thermal properties, flexural properties, impact strength, and morphology of PLA/BS composites were analyzed.

EXPERIMENTAL

1. Materials

PLA pellets with a weight-average molecular weight of 100,000 g/mol were obtained from NatureWorks Co. (USA). Jilin Jinshi New Material Technology Co., Ltd. provided 2-6-μm-thick BS. γ-methacryloxy propyl trimethoxyl silane (KH-570) as a silane coupling agent was purchased from Jinan Xingfeilong Chemical Co., Ltd. Anhydrous ethanol and glacial acetic acid were obtained from Tianjin Damao Chemical Reagent Factory.

2. Surface Treatment of BS

BS (20 g) was dispersed in anhydrous ethanol (400 mL) and glacial acetic acid (80 g) and then ultrasonically treated at 30 °C for 2 h. KH-570 (10 g) and water (10 mL) were added to the mixture, and the mixture was heated to 60 °C and maintained for 1.5 h. Thereafter, the mixture was vacuum-filtered, washed to neutrality, dried at 80 °C for 4 h in a vacuum oven, and ground to obtain surface-treated BS. For convenience, the silane-coupling-agent-modified BS is denoted as KH-BS.

3. Preparation of the Composite Samples

Fig. 1 schematically shows the preparation of the PLA/KH-BS composites. The KH-BS content was varied from 0 to 8 wt%. In a typical procedure, specific amounts of PLA and KH-BS were added to dichloromethane and the mixture was first stirred at 60 °C for 5 min, then stirred at 30 °C for 30 min using a spin stirrer. Subsequently, the mixture was heated to 145 °C in a vacuum oven and injected into a mold sprayed with a mold-release agent. The mixture was then compression-molded at 180 °C under a pressure of 4.5 MPa for 1 h.

4. Characterization and Measurements

The surface morphologies of BS and KH-BS were investigated via HR-SEM (Hitachi, SU 8010). EDX and SEM were used to test for the presence of silicon. The surface properties of BS and KH-BS were evaluated using XPS (Thermo ESCALAB 250) with a monochromatic Al Ka source and a passage energy of 20 eV.

The thermal stability of the PLA/KH-BS composites was evaluated by thermogravimetric analysis (TGA; TA Instruments, Q50) between 30 and 600 °C at a scanning rate of 10 °C/min under nitrogen atmosphere. The glass transition temperature (T_g) of the composites was determined by thermal mechanical analysis (TMA; TA Instruments, Q400) with an applied force of 0.05 N at a heating rate of 5 °C/min under nitrogen atmosphere; the sample size was 5×5×5 mm^3.

The flexural properties of the composites were investigated by three-point bending tests using a mechanical testing apparatus (WDW 3010) according to the GB/T 9341-2008 standard; the sample size was 5×10×80 mm^3. The impact strength of the composites was measured using an Izod impact tester (TP04G-AS1) according to the GB/T 1843-2008 standard; the sample size was 5×10×50 mm^3.

The pristine PLA and PLA/KH-BS composite morphologies were examined using ultrahigh-resolution field emission SEM (HRFE-SEM; TESCAN, MAIA3).

RESULTS AND DISCUSSION

1. Surface Characterization of KH-BS

BS surfaces were treated using a silane coupling agent, and the surface properties were characterized via HR-SEM, EDX, and XPS. Fig. 2 shows the SEM images of pristine BS and KH-BS. BS exhibited a sheet shape with thin thickness and long length and width. The presence of Si on the BS surface after the surface treatment was

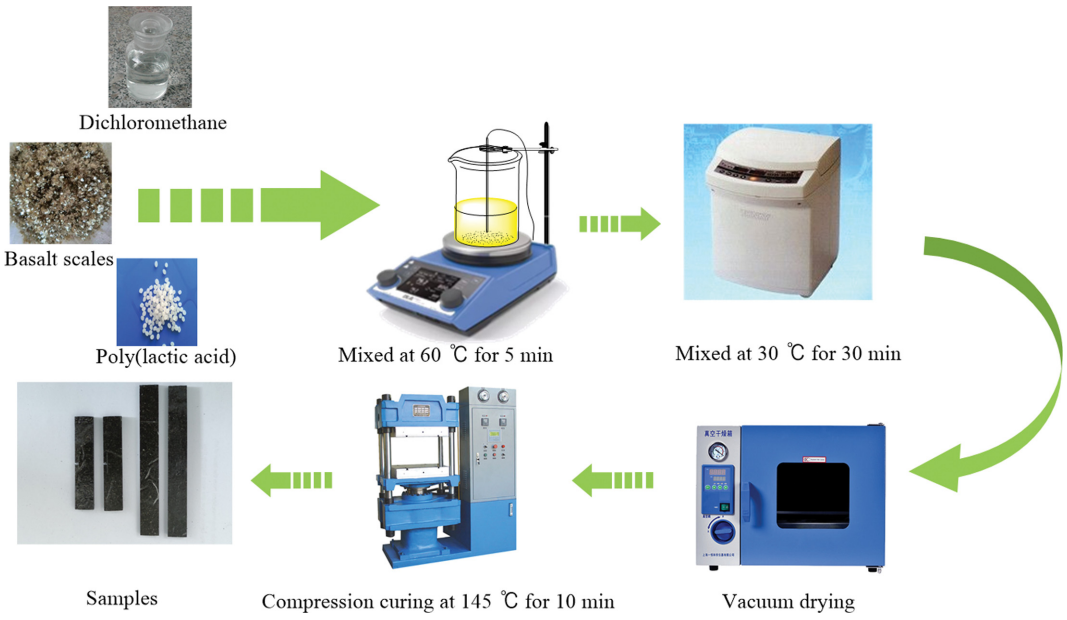

Fig. 1. Schematic illustration of the preparation of PLA/KH-BS composites.

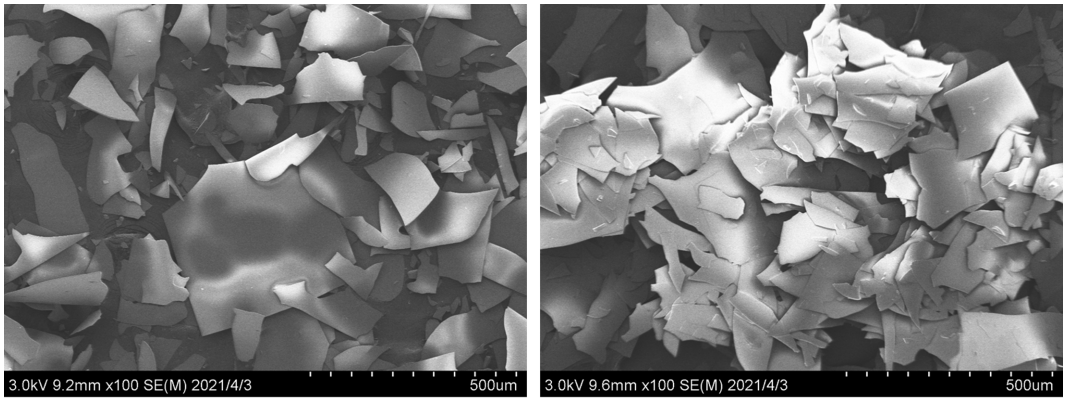

(a) pristine BS (b) KH-BS

Fig. 2. SEM images of pristine BS (a) and KH-BS (b).

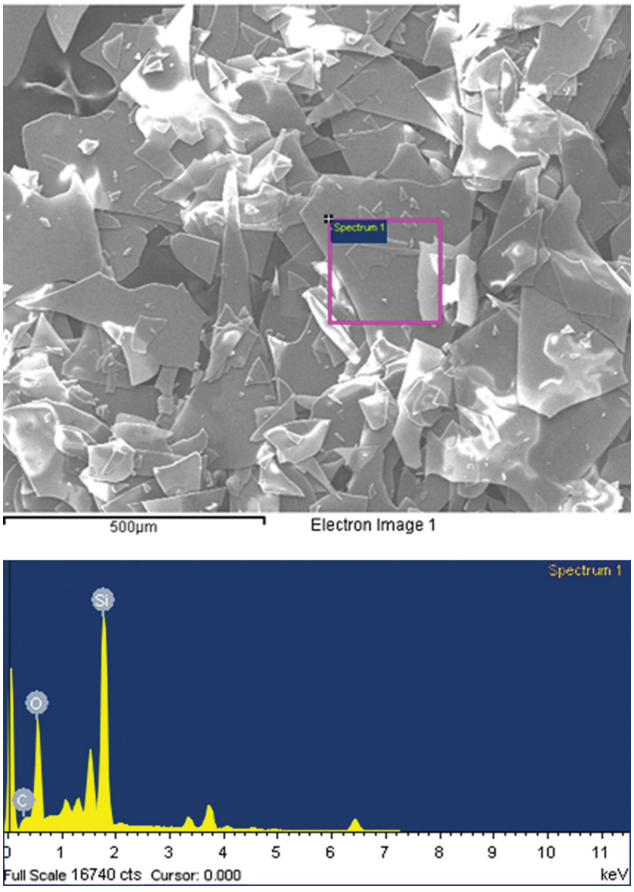

Fig. 3. EDX mapping of surface-treated BS.

confirmed through EDX mapping, as shown in Fig. 3. The peaks at about 0.27, 0.55, and 1.76 keV were ascribed to C, O, and Si, respectively [24,25]. The peaks were afforded due to the reaction of the silane coupling agent with hydroxyl group on the BS surface and introduction of organic functional groups, such as C=O, C-O, and Si-O, on the BS surface after the surface treatment.

The presence of Si on the KH-BS surface was further verified by elemental analysis of the XPS spectra, as shown in Fig. 4. The characteristic peak of C_{1s} was observed at 284.6 eV, and the intensity of the C_{1s} peak increased after the surface treatment with the silane coupling agent. The characteristic peaks of O_{1s} and Si_{2p} were observed at 532.5 and 102.6 eV, respectively, and the intensity of the O_{1s} and Si_{2p} peaks significantly increased after the surface treatment. These results can be explained as follows: BS comprises silicon dioxide, aluminum oxide, iron oxide, calcium oxide, and magnesium oxide. After the silane coupling agent modification, oxygen-containing functional groups, such as C=O, C-O, and Si-O, were introduced on the BS surface [26,27]. Thus, the intensity of the C_{1s}, O_{1s}, and Si_{2p} peaks increased.

2. Thermal Properties of PLA/KH-BS Composites

The thermal properties of pristine PLA and PLA/KH-BS composites were analyzed by TGA and TMA. The thermal degradation of pristine PLA and PLA/KH-BS composites was investigated by TGA, and Fig. 5 shows the results. Moreover, thermal stability factors, such as the initial decomposition temperature (i.e., the temperature of 5% weight loss ($T_{5\%}$)) and the amount of char formation at 600 °C, were calculated using the TGA thermograms [28-30], and Table 1 summarizes the results.

The pristine PLA and PLA/KH-BS composites exhibited thermal degradation and significant weight loss with increasing temperature. Table 1 shows that the $T_{5\%}$ value of the composites increased with the addition of KH-BS. In detail, the $T_{5\%}$ value of the composites was 28-38 °C higher than that of pristine PLA. Furthermore, the amount of char formation at 600 °C increased from 1.8% to 7.5% with increasing KH-BS content from 0 to 8 wt%. This is because BS is extremely thermally stable and has high residual mass (approximately 90 wt%). Additionally, the BS sheets dispersed in the PLA matrix act as a mass transport barrier and yield volatile products during decomposition, increasing the thermal stability of the composites [31,32].

Fig. 6 shows the dimensional changes of the PLA/KH-BS composites measured using TMA under nitrogen atmosphere. Table 1 lists the T_g values determined from the TMA curves. The T_g values of the composites increased with the KH-BS content up to 4 wt%. This is because the introduction of organic functional groups on the BS surface through the silane coupling agent modification increased the interaction between the BS sheets and PLA matrix,

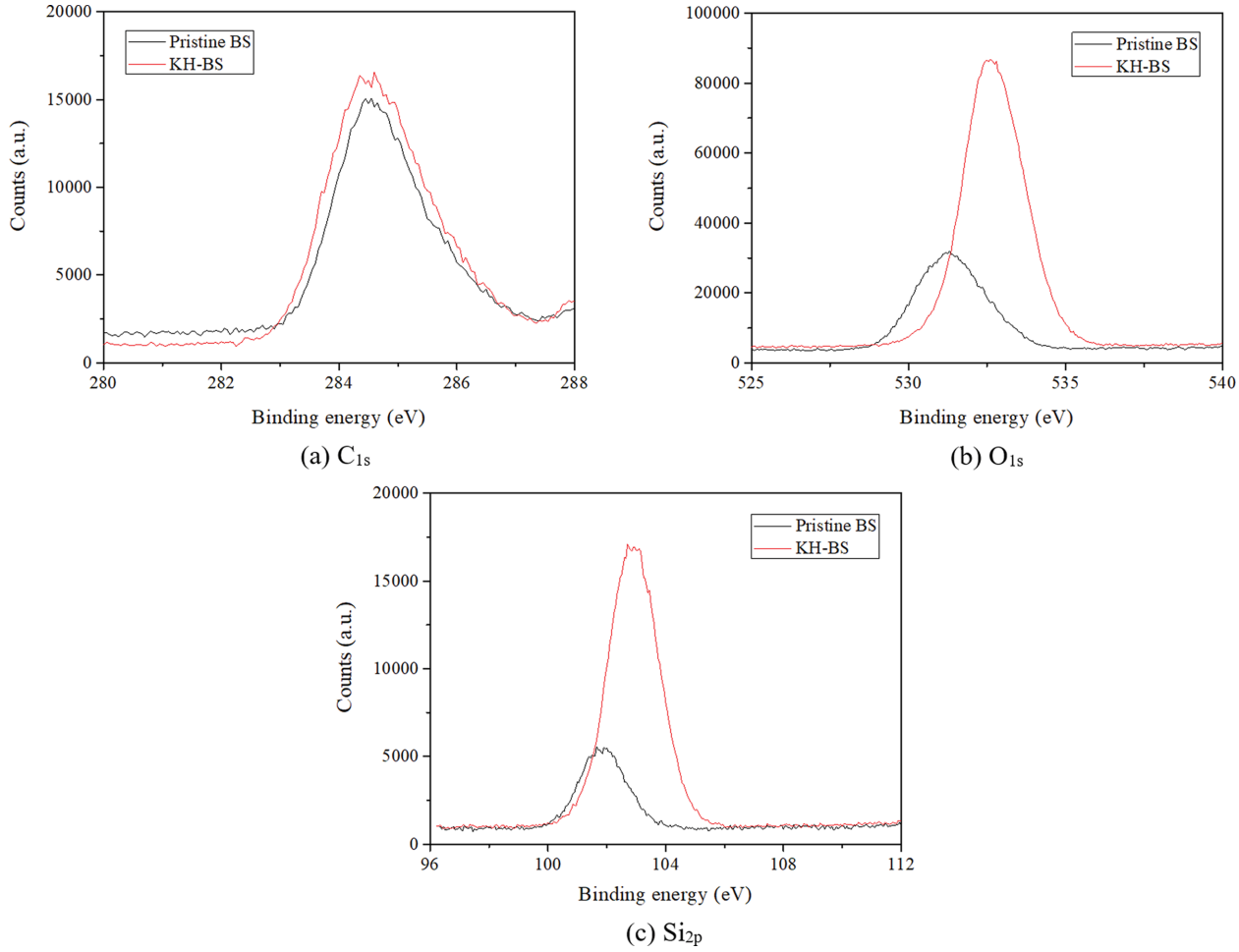

Fig. 4. High-resolution XPS spectra of pristine BS and KH-BS.

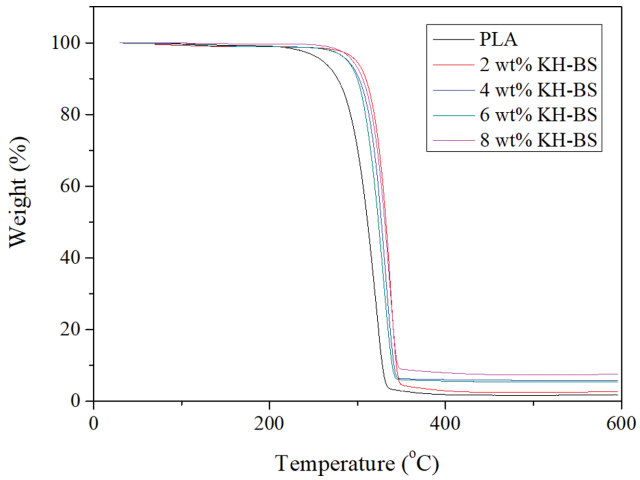

Fig. 5. TGA thermograms of PLA/KH-BS composites as a function of KH-BS fraction.

which consequently reduced the movement of the polymer chains in the composites [31]. The T_g value of the composite with 8 wt% KH-BS was lower than that of pristine PLA, because the dispersion state of the BS sheets in the PLA matrix deteriorated at high KH-BS content [33].

Table 1. Thermal stability factors and T_g of PLA/KH-BS composites

KH-BS content (wt%)	$T_{5\%}$ (°C)[a]	Char at 600 °C (%)[a]	T_g (°C)[b]
0	260.0	1.8	62.02
2	298.4	2.6	68.83
4	288.9	5.7	74.33
6	288.5	5.4	67.38
8	294.4	7.5	57.03

[a]$T_{5\%}$ and char at 600 °C determined from TGA thermograms.
[b]T_g determined from the TMA curves.

3. Flexural Properties of PLA/KH-BS Composites

The flexural properties of the PLA/KH-BS composites were investigated by measuring the flexural strength and modulus. Fig. 7 shows that the flexural strength of the composites decreased with increasing KH-BS content. This indicates that the addition of KH-BS negatively affects the flexural strength. Particularly, the flexural strength of the composite at 8 wt% KH-BS was significantly lower than that of pristine PLA as the BS dispersion state in the PF matrix deteriorated with the addition of high BS contents [34].

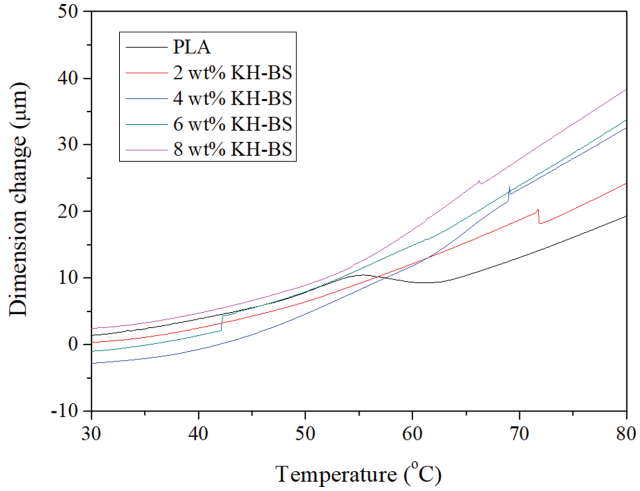

Fig. 6. Dimensional change of PLA/KH-BS composites as a function of KH-BS fraction.

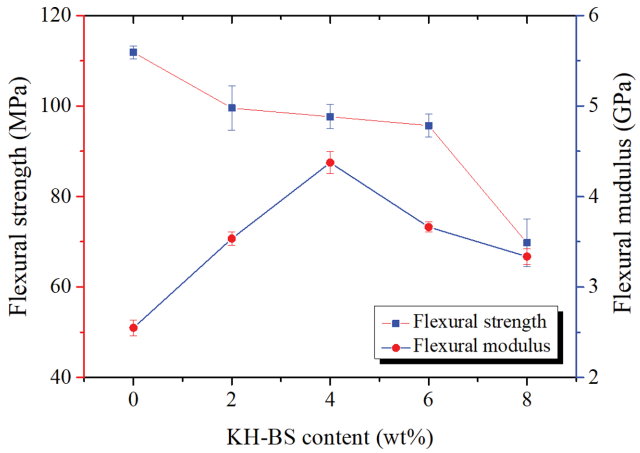

Fig. 7. Flexural strength and flexural modulus of PLA/KH-BS composites.

Fig. 7 demonstrates that the flexural modulus of the PLA/KH-BS composites increased with the addition of KH-BS. Pristine PLA exhibited a flexural modulus of 2.54 GPa. Moreover, the flexural modulus of the composites with 4 wt% KH-BS was 4.37 GPa, which is 72% higher than that of pristine PLA. These results can be attributed to the increase in the stiffness of the composites with the addition of KH-BS, which consequently increases the flexural modulus of the PLA/KH-BS composites [35,36].

4. Impact Strength of PLA/KH-BS Composites

Fig. 8 displays the influence of KH-BS content on the impact strength of the PLA/KH-BS composites. The figure shows that pristine PLA, which is classified as a brittle material, has a low impact strength of 2.07 kJ/m^2 at room temperature. As is known, low impact strength is due to the weak interfacial adhesion between the inorganic particles and polymer matrix. Furthermore, the impact strength increases with the addition of KH-BS. In detail, the impact strength of the composites increased from 2.07 to 2.91 kJ/m^2 for 2 wt% KH-BS (40% increase) and to 3.14 kJ/m^2 for 4 wt% KH-BS (51% increase). The impact strength increase can be attributed to the absorption of external energy by microcracks generated by the KH-BS dispersed in the PLA matrix [37,38]. The impact strength of the PLA/KH-BS composites decreased above 4 wt% KH-BS. Moreover, the impact strength of the PLA/KH-BS composites with 8 wt% KH-BS was lower than that of pristine PLA, which was due to the deterioration of the dispersion state of KH-BS at high KH-BS contents [34].

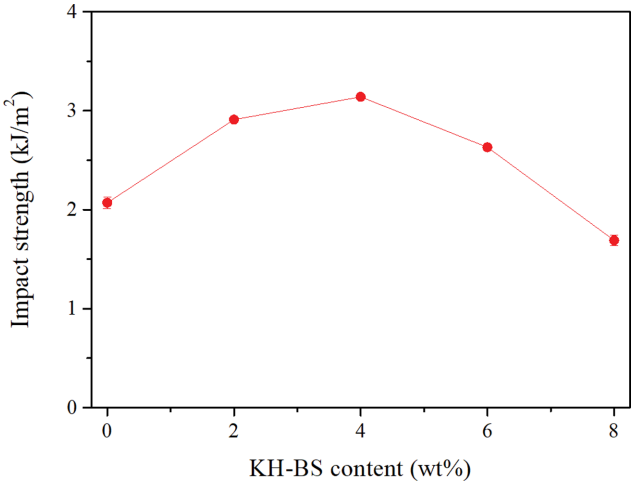

Fig. 8. Impact strength of PLA/KH-BS composites as a function of KH-BS fraction.

5. Morphology of the PLA/KH-BS Composites

The fracture surface morphologies of pristine PLA and PLA/KH-BS composites after the impact strength tests were investigated via SEM, and the SEM images are shown in Fig. 9. Pristine PLA exhibited a smooth and flat morphology with ordered cracking behavior, which indicates brittle deformation prior to fracture [39], as shown in Fig. 9(a). In contrast, the PLA/KH-BS composites containing 2-6 wt% KH-BS exhibited rough morphology with many river-like microcracks, indicating plastic deformation prior to fracture [40,41], as shown in Figs. 9(b)-(d). When the KH-BS content was increased to 8 wt%, the river-like microcracks decreased and the size of fractured cross-section increased, which accounts for its low impact strength, as revealed by the high resolution image in Fig. 9(e).

CONCLUSIONS

Biodegradable PLA/KH-BS composites were prepared via a solution-blending method, and their thermal properties, flexural strength, impact strength, and morphology were investigated. The PLA/KH-BS composites with 4 wt% KH-BS exhibited an initial decomposition temperature of 288.9, which is 11.1% higher than that of pristine PLA; flexural strength of 97.6 MPa, which is 12.7% lower than that of pristine PLA; flexural modulus of 4.37 GPa, which is 72% higher than that of pristine PLA; and an impact strength of 3.14 kJ/m^2, which is 51% higher than that of pristine PLA. Additionally, the SEM results showed that the fracture surfaces of the composites after the impact strength tests exhibited a rough morphology with numerous river-like microcracks.

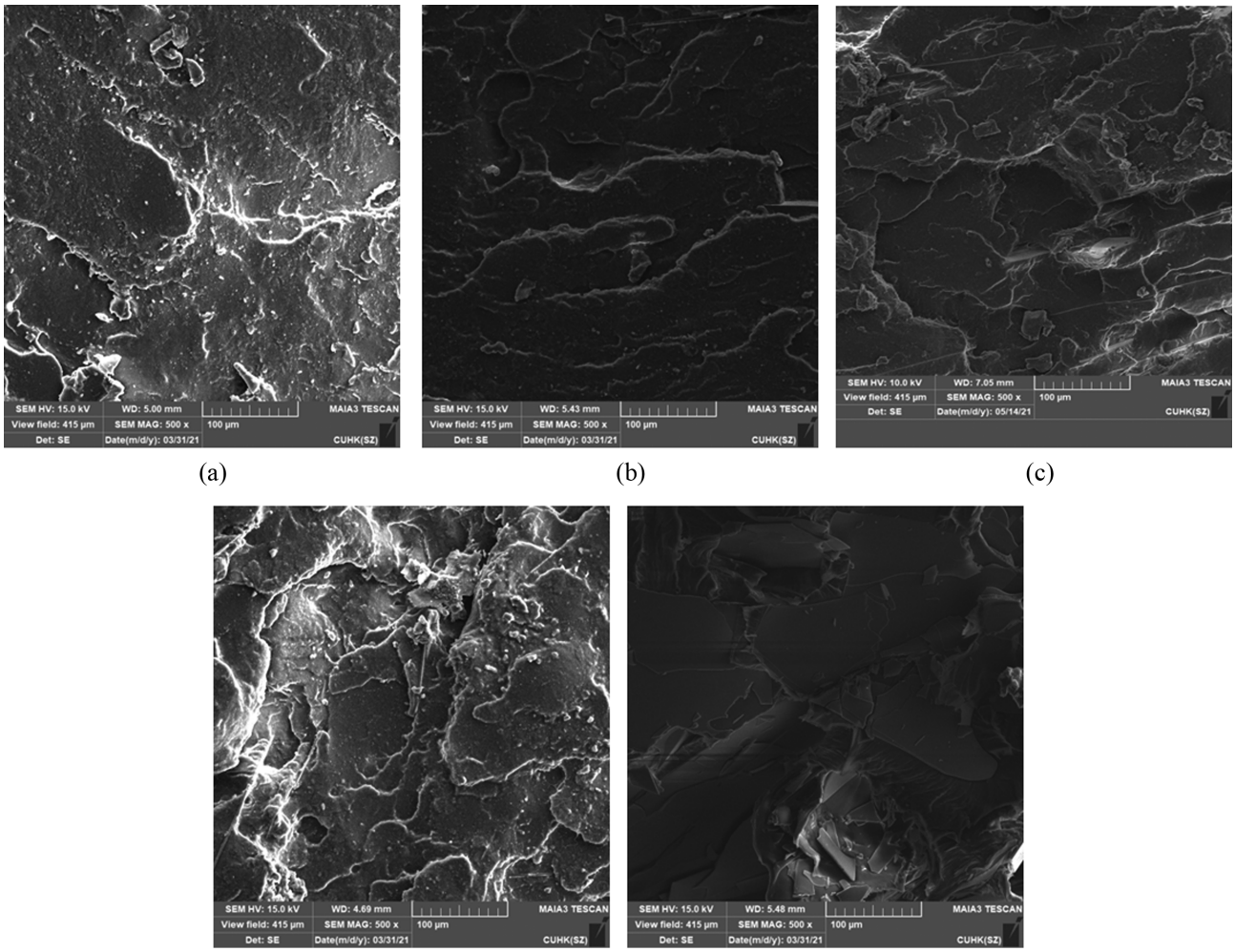

Fig. 9. SEM micrographs of PLA/KH-BS composites: (a) pristine PLA, (b) 2 wt% KH-BS, (c) 4 wt% KH-BS, (d) 6 wt% KH-BS, (e) 8 wt% KH-BS (magnification of 500, scale bar of 100 μm).

ACKNOWLEDGEMENTS

This work was supported by the Technology Innovation Program (or Industrial Strategic Technology Development Program-Development of technology on materials and components) (20010106, Adhesives with low water permeability and low outgassing) funded By the Ministry of Trade, Industry & Energy (MOTIE, Korea).

REFERENCES

1. F. L. Jin, R. R. Hu and S. J. Park, *Compos. Part B-Eng.*, **164**, 287 (2019).
2. A. K. Pandey, H. Takagi, N. Igarashi, N. Shimizu and S. Sakurai, *Polymer*, **229**, 124001 (2021).
3. F. Jiang, D. Yan, J. Lin, H. Kong and Q. Yao, *Mater. Today Chem.*, **21**, 100494 (2021).
4. L. C. Llanes, S. H. Clasen, A. T. N. Pires and I. P. Grossa, *Eur. Polym. J.*, **142**, 110112 (2021).
5. K. Decsov, V. Takács, G. Marosi and K. Bocz, *Polym. Degrad. Stab.*, **191**, 109655 (2021).
6. W. He, L. Ye, P. Coates, F. Caton-Rose and X. Zhao, *J. Mater. Sci. Technol.*, **98**, 186 (2022).
7. T. Péter, K. Litauszki and Á. Kmetty, *Polym. Degrad. Stab.*, **190**, 109646 (2021).
8. F. Yu, X. Fei, Y. He and H. Li, *Int. J. Biol. Macromol.*, **186**, 770 (2021).
9. A. V. Rane, K. Kanny, A. Mathew, M. T. Pandurangan and S. Thomas, *Surf. Interfaces*, **18**, 100451 (2020).
10. J. Liao, N. Brosse, S. Hoppe, X. Zhou, X. Xi, G. Du and A. Pizzi, *Ind. Crop. Prod.*, **159**, 113068 (2021).
11. X. Ge, M. Chang, W. Jiang, B. Zhang, R. Xing and C. Bulin, *Appl. Clay Sci.*, **189**, 105524 (2020).
12. D. Chen and W. Zhen, *Polym. Test.*, **100**, 107232 (2021).
13. S. Liu, S. Qin, M. He, D. Zhou, Q. Qin and H. Wang, *Compos. Part B-Eng.*, **199**, 108238 (2020).
14. H. Zheng, L. Liu, F. Meng, Y. gui, Z. Li, E. E. Oguzie and F. Wang, *J. Mater. Sci. Technol.*, **84**, 86 (2021).
15. H. Zheng, L. Liu, F. Meng, Y. Cui and F. Wang, *Prog. Org. Coat.*, **153**, 106160 (2021).
16. D. Matykiewicz and M. Barczewski, *Compos. Commun.*, **20**, 100360 (2020).
17. S. Q. Liu, Y. Zhang, J. J. Yu, J. Zhang, G. H. Wu, X. L. Yin, P. Wang,

F. Li, M. F. Liu and M. Zhang, *Ind. Textile*, **70**(5), 408 (2019).
18. J. Li, C. Wu, H. Hao, Z. Liu and Y. Yang, *Compos. Struct.*, **203**, 599 (2018).
19. L. E. McGee and I. E. M. Smith, *J. Volcanol. Geoth. Res.*, **325**, 45 (2016).
20. H. He, P. Yang, Z. Duan, Z. Wang and Y. Liu, *Compos. Sci. Technol.*, **199**, 108372 (2020).
21. T. Tábi, A. Z. Égerházi, P. Tamás, T. Czigány and J. G. Kovács, *Compos. Part A-Appl. S.*, **64**, 99 (2014).
22. Z. Ying, D. Wu, M. Zhang and Y. Qiu, *Compos. Struct.*, **176**, 1020 (2017).
23. S. Yu, Y. H. Hwang, J. Y. Hwang and S. H. Hong, *Compos. Sci. Technol.*, **175**, 18 (2019).
24. D. Kurniawan, B. S. Kim, H. Y. Lee and J. Y. Lim, *Compos. Part B-Eng.*, **43**, 1010 (2012).
25. Z. Wang, Y. Liu, H. Lv and B. Yang, *Polym. Compos.*, **39**(9), 3040 (2017).
26. F. L. Jin, C. L. Ma, B. T. Guo and S. J. Park, *Bull. Korean Chem. Soc.*, **40**(10), 991 (2019).
27. M. J. Kang, F. L. Jin and S. J. Park, *Macromol. Res.*, **26**(11), 1048 (2018).
28. J. Chen, R. R. Hu, F. L. Jin and S. J. Park, *J. Appl. Polym. Sci.*, **138**(16), 50250 (2021).
29. F. L. Jin, Q. Q. Pang, T. Y. Zhang and S. J. Park, *J. Ind. Eng. Chem.*, **32**(1), 77 (2015).
30. S. S. Yao, C. L. Ma, F. L. Jin and S. J. Park, *Korean J. Chem. Eng.*, **37**(11), 2075 (2020).
31. M. Barczewski, K. Lewandowski, D. Rybarczyk and A. Klozinski, *Polym. Test.*, **91**, 106768 (2020).
32. D. Matykiewicz, M. Barczewski and S. Michałowski, *Compos. Part B-Eng.*, **164**, 272 (2019).
33. J. B. Zhang, H. Zhang, F. L. Jin and S. J. Park, *Bull. Mater. Sci.*, **43**, 6 (2020).
34. H. Wang, S. S. Yao, Z. Guan, F. L. Jin and S. J. Park, *Korean J. Chem. Eng.*, **38**(11), 2332 (2021).
35. M. Barczewski, O. Mysiukiewicz, K. Lewandowski, D. Nowak, D. Matykiewicz, J. Andrzejewski, K. Skórczewska and A. Piasecki, *Materials*, **13**, 5436 (2020).
36. M. Barczewski, O. Mysiukiewicz, D. Matykiewicz, A. Kloziński, J. Andrzejewski and A. Piasecki, *Polym. Test.*, **89**, 106628 (2020).
37. A. Zotti, S. Zuppolini, T. Tábi, M. Grasso, G. Ren, A. Borriello and M. Zarrelli, *Compos. Part B-Eng.*, **153**, 364 (2018).
38. S. Kuciel, K. Mazur and M. Hebda, *J. Polym. Environ.*, **28**, 1204 (2020).
39. F. L. Jin, H. Zhang, S. S. Yao and S. J. Park, *Macromol. Res.*, **26**(3), 211 (2018).
40. S. S. Yao, Q. Q. Pang, R. Song, F. L. Jin and S. J. Park, *Macromol. Res.*, **24**(11), 961 (2016).
41. F. L. Jin, R. R. Hu and S. J. Park, *Korean J. Chem. Eng.*, **37**(5), 905 (2020).